

The influence of chemical structure on the friction properties between particles and compacted powder surfaces

F. PODCZECK, J. M. NEWTON

Department of Pharmaceutics, The School of Pharmacy, University of London, 29/39 Brunswick Square, London WC1N 1AX, UK

M. B. JAMES

Glaxo Research & Development Ltd., Park Road, Ware, Herts SG12 0DP, UK

Friction measurements on particles adhered to compacted powder surfaces have been undertaken by the centrifuge technique to investigate the influence of the variations in the chemical structure of a series of salts of salmeterol. Two mathematical models have been used to evaluate the experiments, and the coefficient of static friction, the friction force and the theoretical shear force on compacted powder surfaces of lactose monohydrate and salmeterol xinafoate have been derived. The results show differences in the mechanism of friction and also divide the five compounds into comparatively hard (salmeterol base and sulfate) and soft (salmeterol 4-chlorobenzoate, salicylate and xinafoate) materials. The hydrophilic nature of the particulate material was found to be indicative of its friction properties on a hydrophobic surface, and vice versa. The ability of a material to adsorb water is reflected in the relative hydrogen bonding coefficient (Hansen-solubility parameter), and a linear relationship was found between this coefficient and the friction force obtained. Water can act as a lubricant reducing the friction between two surfaces. The friction between like materials in contact was found to be minimal. The results also imply that no general descriptor of the chemical structure of related compounds, which would allow the prediction of friction properties, exists. Instead, the descriptor needs to be chosen according to the properties of the surfaces in contact, or friction experiments have to be performed.

1. Introduction

During the manufacture of dry powder inhalation applications, adhesion and friction occur between the carrier and drug particles influencing the homogeneity of the mixtures and their subsequent handling properties during inhalation. During powder mixing, sliding friction will dominate over static phenomena, whereas during the inhalation process the larger static friction forces, which occur during the detachment of the drug particles from the carrier particles, act in addition to adhesion forces. It has been shown previously [1–3] that a centrifuge technique can be successfully used to determine static friction forces and the coefficient of static friction between particles and a surface of flat or particulate nature.

Mechanical properties of the contacting bodies are important in the prediction of friction forces. Differences in material hardness lead to different types of abrasion, and the ductility or brittleness of the softer surface also effects the friction result [4]. DeCelis [5] quantified the relationship between fracture toughness, hardness and coefficient of dynamic friction for ductile and brittle materials in autoadhesion contact.

Particular attention has been drawn to the effect of surface roughness on friction phenomena. An asperity based model was developed by Greenwood and Williamson [6], which is still the basic assumption involved in friction studies [7]. This model defines the shape, radius and height of the asperities and their distance from each other, and it assumes that only the asperities deform during the surface contact. The relative movement of the contacting surfaces will not start simultaneously at all asperity contact points (“micro-displacement phenomenon”, Bowden and Tabor [8]). The influence of the degree of surface roughness on the micro-displacement can be described statistically [9]. Generally, friction is lowest between highly polished surfaces, and it increases with increased surface roughness. However, for extremely rough surfaces ($R_q > 2.5 \mu\text{m}$) it was found that the friction phenomena are independent of the actual surface roughness value [10]. To date, no link has been made between the chemical structure of organic powders in contact and the friction phenomena.

The aim of this work was to assess the friction force and the coefficient of static friction for a series of

related chemicals (salmeterol base and four salmeterol salts), and to identify key points in their chemical structure, which might give a predictive link to the friction properties measured on compacted powder surfaces.

The following two models used require the measurement of a median detachment force of particles adhered to a surface using different angles between the detachment force vector (in this paper a centrifuge force vector) and the surface.

Model I [2] allows the calculation of the coefficient of static friction μ from the following linear function

$$F_{\text{det}} \cos \alpha = -\mu F_{\text{det}} \sin \alpha + \mu F_{\text{ad}} \quad (1)$$

where F_{det} is the median detachment force, α is the angle between the detachment force vector and the surface, and F_{ad} is the median adhesion force. The friction force F_{frict} is equal to the intercept ($\mu \times F_{\text{ad}}$) of the function. Model II [1] calculates a force value F_s that results from the two forces (F_{ad} and F_{det}) which pull on the particles during detachment in different directions

$$F_s = [F_{\text{ad}}^2 + F_{\text{det}}^2 - 2F_{\text{ad}}F_{\text{det}} \cos(90^\circ + \alpha)]^{1/2} \quad (2)$$

From the linear function of $F_s = f(\alpha)$ a shear force F_{shear} (intercept) can be calculated, which is (a) equal to F_{det} at $\alpha = 0^\circ$ if adhesion does not take part in the friction process, (b) equal to F_{ad} if adhesion is the main mechanism to resist the friction force, or (c) larger than F_{ad} if other mechanisms such as ploughing are also involved. In the latter case, the difference between F_{shear} and F_{ad} quantifies the ploughing component.

2. Experimental procedure

Salmeterol base and its salts, 4-chlorobenzoate, sulfate and salicylate have been used as unfractionated powder samples. Salmeterol xinafoate has been used as a particle size fraction $< 90 \mu\text{m}$. The particle size distribution was determined using image analysis (Seescan Solitaire 512) of particles suspended in liquid paraffin. Two drops of the homogeneous suspension were placed on a glass slide and covered with a cover slip allowing the suspension to be equally distributed between the two glass surfaces. One thousand particles were measured per sample, and the mean Feret diameter of the number distribution was determined. The materials have the following mean Feret diameters: $15.4 \pm 12.5 \mu\text{m}$ (base), $14.7 \pm 7.4 \mu\text{m}$ (sulfate), $19.6 \pm 15.9 \mu\text{m}$ (4-chlorobenzoate), $22.7 \pm 15.7 \mu\text{m}$ (salicylate) and $35.9 \pm 27.2 \mu\text{m}$ (xinafoate). To determine the particle mass, particles were sprinkled onto dark grey plastic discs using a $45 \mu\text{m}$ (salmeterol base and sulfate) or $63 \mu\text{m}$ sieve. The sieve sizes were chosen to match the most frequent particle size identified in the particle size analyses of the powders and to exclude agglomerates. The total particle mass was assessed by difference weighing using an autobalance (AD-4, Perkin Elmer). The number of particles per disc was then counted using image analysis. These measurements were replicated four

times. The following particle masses were determined: $37.7 \pm 3.6 \text{ ng}$ (base), $37.4 \pm 19.3 \text{ ng}$ (sulfate), $55.8 \pm 18.2 \text{ ng}$ (4-chlorobenzoate), $35.7 \pm 4.1 \text{ ng}$ (salicylate) and $64.0 \pm 8.2 \text{ ng}$ (xinafoate).

Lactose monohydrate and salmeterol xinafoate were chosen as powder surfaces in the compacted form. Such compacted surfaces need to be very stress resistant against high centrifuge forces applied in the adhesion/friction experiments. Hence, bilayer surfaces of the powders with microcrystalline cellulose as support surface were made, using either 360 mg microcrystalline cellulose and 50 mg salmeterol xinafoate (top layer) or 330 mg microcrystalline cellulose and 100 mg lactose monohydrate (top layer). The amount of microcrystalline cellulose was weighed and poured into a 12.77 mm punch and split-die system levelling the powder surface horizontally using first a spatula and then a 12.77 mm punch surface without application of any measurable pressure. The powder bed did not exceed the maximum bulk density at this stage. The amount of salmeterol xinafoate or lactose monohydrate was spread on top of the support powder layer and distributed equally. The upper punch was fitted and the punch and die system was placed between the two plates of a Universal Testing Machine (Instron, Model TT). The necessary compaction pressure (80 MPa) was applied using a cross-head speed of 0.05 mm s^{-1} . Afterwards, punch and die were disassembled, and the compacts which had formed were stored in Petri dishes at 35% relative humidity of the air for at least eight weeks. The top layer was approximately $400 \mu\text{m}$ thick, and the final dimensions of the compacts were 12.9 mm diameter and 2.95 mm height.

Powder particles were deposited on top of the active layer of the compacted surfaces using a sieve technique to guarantee an agglomeration-free distribution. The adhesion and friction properties of these particles were assessed with the centrifuge technique described earlier [3] based on the Ultracentrifuge Centrikon T-1080 using a vertical rotor (TV-850, DuPont Sourvall) and a set of specially devised adapters. A press-on force of about $5 \times 10^{-9} \text{ N}$ was used, and several spin-off forces were applied to obtain adhesion force distributions, from which the median detachment force for the friction experiments (median adhesion force in adhesion experiments) was obtained. Additionally, the interquartile range of the adhesion force was assessed to describe the shape of the distributions. All results quoted are the arithmetic mean value and standard deviation of six compacted surfaces tested.

3. Results and discussion

Table I summarizes the median adhesion/friction forces and interquartile ranges obtained for the salmeterol compounds on compacted lactose monohydrate surfaces. The value of α is the angle between the centrifuge force vector and the compacted powder surface. Consequently, an α value of 90° is equivalent to the classical adhesion experiment [11], whereas an α value below 90° has been used in classical friction studies [12]. The measurement of the median adhesion

TABLE I Adhesion and friction forces measured between particles of salmeterol compounds and compacted lactose monohydrate surfaces (arithmetic mean \pm standard deviation)

Salmeterol	F_{on}	$\alpha = 90^\circ$	$\alpha = 80^\circ$	$\alpha = 60^\circ$	$\alpha = 40^\circ$	$\alpha = 20^\circ$	$\alpha = 0^\circ$
Base	4.92 <i>M</i>	2.58 \pm 0.54	1.90 \pm 0.21	1.88 \pm 0.26	0.76 \pm 0.07	0.81 \pm 0.13	0.76 \pm 0.09
	IQR	3.61 \pm 0.81	1.69 \pm 0.11	2.03 \pm 0.12	1.01 \pm 0.17	1.03 \pm 0.22	1.02 \pm 0.23
Sulfate	4.88 <i>M</i>	3.05 \pm 0.24	3.54 \pm 0.19	1.70 \pm 0.21	1.17 \pm 0.20	0.84 \pm 0.06	0.73 \pm 0.04
	IQR	4.70 \pm 0.66	3.72 \pm 0.72	1.94 \pm 0.19	1.48 \pm 0.10	0.76 \pm 0.11	0.53 \pm 0.04
4-Cl-benzoate	5.22 <i>M</i>	2.24 \pm 0.35	1.47 \pm 0.13	1.35 \pm 0.15	1.47 \pm 0.18	1.06 \pm 0.06	0.67 \pm 0.17
	IQR	2.83 \pm 0.24	1.82 \pm 0.24	1.67 \pm 0.28	1.74 \pm 0.31	1.20 \pm 0.17	0.89 \pm 0.08
Salicylate	4.66 <i>M</i>	1.69 \pm 0.16	1.21 \pm 0.16	0.88 \pm 0.07	0.71 \pm 0.04	0.67 \pm 0.02	0.56 \pm 0.07
	IQR	1.78 \pm 0.29	0.87 \pm 0.06	0.69 \pm 0.06	0.72 \pm 0.06	0.65 \pm 0.06	0.59 \pm 0.06
Xinafoate	4.94 <i>M</i>	1.01 \pm 0.09	0.83 \pm 0.09	0.68 \pm 0.13	0.52 \pm 0.17	0.55 \pm 0.15	0.59 \pm 0.08
	IQR	1.11 \pm 0.38	0.87 \pm 0.22	n.d.	n.d.	n.d.	n.d.

M, median detachment force ($\times 10^{-9}$ N); IQR, interquartile range ($\times 10^{-9}$ N); α , angle between centrifugal vector and surface; F_{on} , press-on force ($\times 10^{-9}$ N); n.d., value not determined, because initial amount of particles detached was below 75%.

TABLE II Adhesion and friction forces measured between particles of salmeterol compounds and compacted salmeterol xinafoate surfaces (arithmetic mean \pm standard deviation)

Salmeterol	F_{on}	$\alpha = 90^\circ$	$\alpha = 80^\circ$	$\alpha = 60^\circ$	$\alpha = 40^\circ$	$\alpha = 20^\circ$	$\alpha = 0^\circ$
Base	4.92 <i>M</i>	3.54 \pm 0.45	3.82 \pm 0.76	2.48 \pm 0.34	3.06 \pm 0.24	2.26 \pm 0.44	2.18 \pm 0.37
	IQR	5.35 \pm 0.67	5.46 \pm 0.83	3.30 \pm 0.38	4.14 \pm 0.30	3.51 \pm 0.66	4.52 \pm 0.54
Sulfate	4.88 <i>M</i>	3.01 \pm 0.24	2.82 \pm 0.19	2.23 \pm 0.67	2.33 \pm 0.22	2.10 \pm 0.32	1.42 \pm 0.25
	IQR	3.33 \pm 0.21	4.11 \pm 0.87	2.68 \pm 0.44	2.69 \pm 0.42	3.04 \pm 0.38	2.43 \pm 0.27
4-Cl-benzoate	5.22 <i>M</i>	3.86 \pm 0.67	3.70 \pm 0.46	2.76 \pm 0.39	2.89 \pm 0.19	1.94 \pm 0.44	1.13 \pm 0.18
	IQR	4.59 \pm 0.73	4.72 \pm 0.32	4.13 \pm 0.78	3.83 \pm 0.29	2.25 \pm 0.36	2.07 \pm 0.45
Salicylate	4.66 <i>M</i>	2.36 \pm 0.19	2.22 \pm 0.23	1.86 \pm 0.23	0.97 \pm 0.10	0.99 \pm 0.08	0.62 \pm 0.05
	IQR	2.32 \pm 0.55	2.22 \pm 0.34	2.27 \pm 0.26	1.00 \pm 0.06	1.15 \pm 0.09	0.73 \pm 0.10
Xinafoate	4.94 <i>M</i>	2.12 \pm 0.17	2.03 \pm 0.22	1.18 \pm 0.11	1.03 \pm 0.12	0.86 \pm 0.08	0.67 \pm 0.05
	IQR	2.57 \pm 0.51	2.36 \pm 0.43	1.47 \pm 0.13	1.27 \pm 0.22	0.99 \pm 0.13	n.d.

M, median detachment force ($\times 10^{-9}$ N); IQR, interquartile range ($\times 10^{-9}$ N); α , angle between centrifugal vector and surface; F_{on} , press-on force ($\times 10^{-9}$ N); n.d., value not determined, because initial amount of particles detached was below 75%.

force ($\alpha = 90^\circ$) is necessary for the calculations based on model II considered in the theoretical section. Table II lists similar values for the observations made on compacted salmeterol xinafoate surfaces.

For salmeterol base on compacted lactose monohydrate surfaces, any median detachment force between α of 90 to 40° is less than its predecessor at a higher α value. Between 40 and 0° the median detachment force appears to be relatively constant. This suggests that in a classical macroscopic friction experiment e.g. using a slope, the transition angle between static and dynamic friction would be found between an angle of decline of 40 and 60° . For the same powder material on compacted salmeterol xinafoate surfaces, generally all median detachment force values are higher than the comparative values for compacted lactose monohydrate surfaces. At an angle α of 80° there is a slight increase in median detachment force compared to the median adhesion force suggesting a stick-slip motion [13] rather than an immediate, smooth detachment. This might have resulted in greater surface damage compared to a smooth detachment [14], because the major causes of surface damage due to friction are the breaking of adhesion junctions and the deformation of the asperi-

ties in adhesion contact. In systems such as those studied, where the adhesion force has been enhanced (press-on force applied) to obtain maximal surface contact, these phenomena are likely to be found and have to be considered in the later stage when using friction models to assess the coefficient of static friction and the degree of ploughing. The angle of decline for the transition between static and dynamic friction appears to be between 80 and 60° , hence larger than for the same chemical on compacted lactose monohydrate surfaces.

For salmeterol sulfate particles, stick-slip motion appears to occur on the compacted lactose monohydrate surfaces (see Table I) but not on the compacted salmeterol xinafoate surfaces (see Table II). In both cases the angle of transition between static and dynamic friction is suggested to lie between 80 and 60° . The adhesion of the particles to either surface is statistically not different, but the median detachment forces for α values between 60 and 0° are higher for compacted salmeterol xinafoate surfaces suggesting larger friction effects.

Comparing the results obtained from the detachment force distributions for salmeterol 4-chlorobenzoate particles adhered to compacted surfaces of

lactose monohydrate (see Table I) and salmeterol xinafoate (see Table II), a smooth detachment occurs in both cases, reflected in the consecutive decline of the median detachment forces with decreasing angle α . The angle of transition between static and dynamic friction is approximately between 40 and 20°. In general the force values obtained on compacted salmeterol xinafoate surfaces are higher than those obtained on compacted lactose monohydrate surfaces.

Salmeterol salicylate particles, when tested on compacted lactose monohydrate (see Table I) and salmeterol xinafoate surfaces (see Table II), again provide a steady decline in the median detachment force when decreasing the angle between the centrifuge force vector and the compacted surface. The detachment force values obtained on the compacted salmeterol xinafoate surfaces are higher than those resulting from the experiments undertaken with compacted lactose monohydrate surfaces. For the experiments using compacted lactose monohydrate surfaces the angle of transition between static and dynamic friction cannot be determined. However, using compacted salmeterol xinafoate surfaces this angle appears to be between 60 and 40°.

Salmeterol xinafoate provides the least adhering particulate material to either surface tested (see Tables I and II). The results suggest a generally smooth detachment and stronger (auto)adherence to compacted salmeterol xinafoate surfaces. The latter is in agreement with previous findings [15,16]. The angle of transition between static and dynamic friction is approximately 60–40° and 80–60° using compacted lactose monohydrate and compacted salmeterol xinafoate surfaces, respectively.

Based on the median detachment forces provided in Tables I and II the coefficient of static friction and the friction force between particles and surfaces has been calculated using model I (see Section 1 and Table III). Fig. 1(a) shows this model function for salmeterol xinafoate particles adhered to compacted lactose monohydrate surfaces as an example. Furthermore, a theoretical adhesion force has been derived from the

TABLE III Coefficient of static friction based on friction model I, and related values for salmeterol compounds adhered to compacted lactose monohydrate and salmeterol xinafoate surfaces

Surface	Salmeterol	μ	F_{frict}	$F_{\text{ad(t)}}$
Lactose monohydrate	Base	0.28	0.78 ± 0.05	2.76
	Sulfate	0.25	0.93 ± 0.16	3.73
	4-Cl-benzoate	0.62	1.37 ± 0.25	2.22
	Salicylate	0.44	0.74 ± 0.02	1.70
	Xinafoate	0.57	0.61 ± 0.03	1.07
Salmeterol xinafoate	Base	0.54	2.34 ± 0.27	4.36
	Sulfate	0.87	2.79 ± 0.27	3.23
	4-Cl-benzoate	0.59	2.67 ± 0.54	4.55
	Salicylate	0.28	0.84 ± 0.15	3.03
	Xinafoate	0.39	0.99 ± 0.12	2.51

μ , coefficient of static friction; F_{frict} , friction force ($\times 10^{-9}$ N) (arithmetic mean \pm standard deviation, $F_{\text{ad(t)}}$, theoretical adhesion force ($\times 10^{-9}$ N).

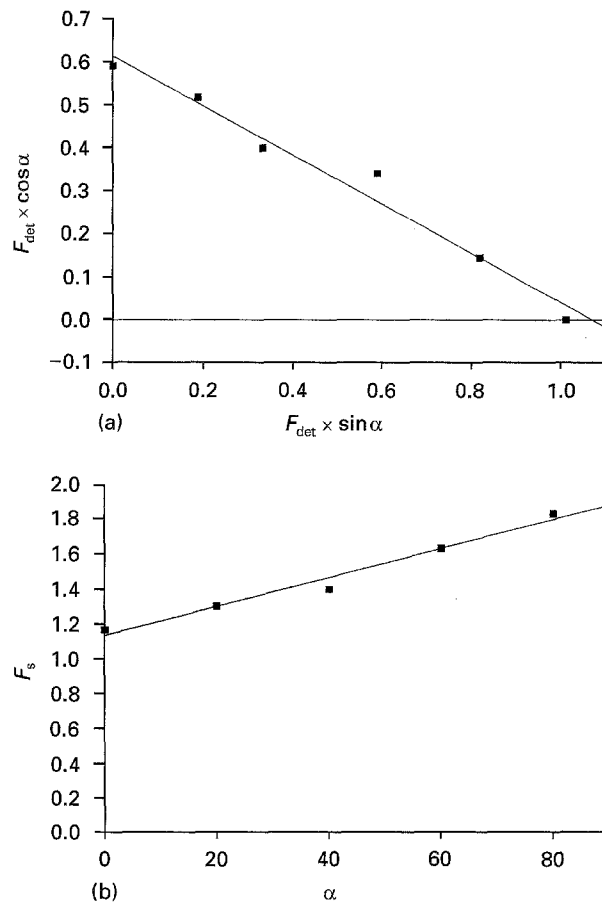


Figure 1 The use of friction models (see Section 1) to estimate the coefficient of static friction (a) and the theoretical shear force (b) for salmeterol xinafoate particles adhered to compacted lactose monohydrate surfaces. F_{det} , median detachment force; F_s , force that pulls on the particles in friction tests (centrifuge technique).

intercepts of the numerical equations. The theoretical and practically measured adhesion force values would be identically if adhesion was the only source of friction observed. However, for the measurements of salmeterol sulfate on compacted lactose monohydrate surfaces, and for salmeterol base, salicylate and xinafoate on compacted salmeterol xinafoate surfaces the values are statistically significantly different (t -test: $t_{P=0.05} = 2.57$, $t_{\text{sulfate/lactose}} = 6.34$, $t_{\text{base/xinafoate}} = 4.07$, $t_{\text{salicylate/xinafoate}} = 7.88$, $t_{\text{xinafoate/xinafoate}} = 5.13$). As mentioned previously there is considerable stick-slip motion between salmeterol sulfate particles and compacted lactose monohydrate surfaces, as well as between salmeterol base particles and compacted salmeterol xinafoate surfaces, probably causing a larger degree of surface damage and surface removal (ploughing effect, Bowden and Tabor [17]). It can therefore be assumed that the higher values of the adhesion force estimated using model I are in all cases the result of considerable surface damage during friction.

The coefficient of static friction is higher on compacted salmeterol xinafoate surfaces for salmeterol base and sulfate only, whereas for the three other salts the values obtained on compacted lactose monohydrate surfaces are higher although the median detachment forces were generally lower. Compacted lactose monohydrate provides the rougher and

harder surfaces (root mean square of rugosity: $R_q = 2.8 \pm 0.3 \mu\text{m}$; indentation hardness: $H = 420 \text{ MPa}$ [18]). However, only the hardness of the surfaces appears to be important. The roughness of the compacted surfaces is higher than the value of $R_q = 2.5 \mu\text{m}$ given in the literature [10] as a maximum roughness, above which the surface roughness no longer influences the friction. Assuming that hard abrasion is the more common phenomenon in friction [4], the results indicate that salmeterol base and sulfate are very hard materials which damage the compacted salmeterol xinafoate surfaces when in friction contact. On the other hand, the hard lactose monohydrate asperities might pull off pieces of the rather soft particles of the other three salmeterol salts, and finally some soft abrasion between these three salmeterol salts and the compacted salmeterol xinafoate surfaces could occur, possibly damaging both the particulate and the compacted surfaces.

The theoretical shear forces calculated using model II (see theoretical section) are listed in Table IV, and Fig. 1(b) shows the graphical presentation of this model function for salmeterol xinafoate particles adhered to compacted lactose monohydrate surfaces as an example. Again a theoretical adhesion force could be derived and compared statistically with the measured median adhesion forces (see Tables I and II). In two cases there is a significant difference (t -test: $t_{P=0.05} = 2.57$, $t_{\text{sulfate/xinafoate}} = 2.65$, $t_{\text{salicylate/xinafoate}} = 2.71$). This is the first indication that mechanisms other than adhesion are involved in the friction process. The comparison of the theoretical shear forces with the measured median adhesion forces is also indicative of ploughing. With the exception of salmeterol base and 4-chlorobenzoate adhered to compacted lactose monohydrate surfaces and salmeterol 4-chlorobenzoate adhered to compacted salmeterol xinafoate surfaces, all theoretical shear forces are significantly higher than the measured median adhesion forces (t -test for comparable variances, Welch-Aspin test for variance inhomogeneity). For the three exceptional cases there was also no obvious ploughing detected using model I. Hence in these three samples, adhesion is the main factor causing friction, if the surfaces are in motion.

TABLE IV Theoretical shear force between compacted surfaces of lactose monohydrate and salmeterol xinafoate and particles of salmeterol compounds, based on friction model II

Surface	Salmeterol	F_{shear}	$F_{\text{ad(t)}}$
Lactose monohydrate	Base	2.86 ± 0.16	2.76
	Sulfate	3.37 ± 0.22	3.29
	4-Cl-benzoate	2.43 ± 0.06	2.34
	Salicylate	1.87 ± 0.08	1.78
	Xinafoate	1.20 ± 0.03	1.04
Salmeterol xinafoate	Base	4.31 ± 0.16	3.72
	Sulfate	3.57 ± 0.18	3.27
	4-Cl-benzoate	4.35 ± 0.27	4.20
	Salicylate	2.65 ± 0.18	2.57
	Xinafoate	2.39 ± 0.17	2.29

F_{shear} , theoretical shear force ($\times 10^{-9}$ N) (arithmetic mean \pm standard deviation); $F_{\text{ad(t)}}$, theoretical adhesion force ($\times 10^{-9}$ N).

To find out whether or not there are parts of the chemical structure, which might be responsible for the different friction behaviour, the molecular structure of the chemicals was quantified using Hansen's solubility parameter approach [19, 20]. This approach is based on the reconstruction of the chemical structure from homomorph components and functional groups. (Homomorph components are chemicals which have a similar basic structure but different functional groups. For example, cyclohexane, methylcyclohexane and cyclohexylamine are homomorph components, because the basic structure is cyclohexane.) For the homomorph components and the functional groups, the Hansen-solubility parameters are tabulated. The tabulated values can be used for the calculation of the solubility parameters of any further chemical structure using the equations provided by Hansen and Beerbower [20].

Table V lists the Hansen-solubility parameters for the salmeterol compounds as relative values. The relative dispersion coefficient D characterizes the hydrophobic properties of a chemical, whereas the relative polarity coefficient P and the relative hydrogen bonding coefficient H describe the hydrophilic character of a substance regarding its overall polarity and its particular affinity to H-bondings, respectively. The salmeterol compounds are comparatively apolar when compared to lactose monohydrate, which is characterized by the following Hansen-solubility parameters: $P = 64.82\%$, $H = 71.82\%$, $D = 25.32\%$. Hence the friction measurements undertaken reflect friction behaviour of comparatively apolar particulate materials on (a) polar, hydrophilic surfaces (compacted lactose monohydrate) and (b) apolar, hydrophobic surfaces (compacted salmeterol xinafoate).

Fig. 2 compares the coefficient of static friction obtained on compacted lactose monohydrate and salmeterol xinafoate surfaces with the relative polarity coefficient of the salmeterol compounds. On the hydrophilic compacted lactose monohydrate surface a maximum coefficient of static friction exists between 34 and 35% relative polarity of the adhered particles. On the other hand, a minimum coefficient of static friction was obtained at a relative polarity of about 31.5% of the salmeterol compounds adhered onto the hydrophobic compacted salmeterol xinafoate surfaces. Salmeterol salicylate and salmeterol xinafoate are similar in terms of their polarity. Hence, it could be concluded that the static friction between like substances has the lowest value.

TABLE V Hansen-solubility parameters for salmeterol compounds

Salmeterol	D (%)	P (%)	H (%)
Base	73.29	29.00	61.57
Sulfate	71.44	36.29	59.85
4-Chlorobenzoate	72.27	34.62	59.79
Salicylate	69.93	31.48	64.17
Xinafoate	69.55	31.70	64.50

D , relative dispersion coefficient; P , relative polarity coefficient; H , relative hydrogen bonding coefficient.

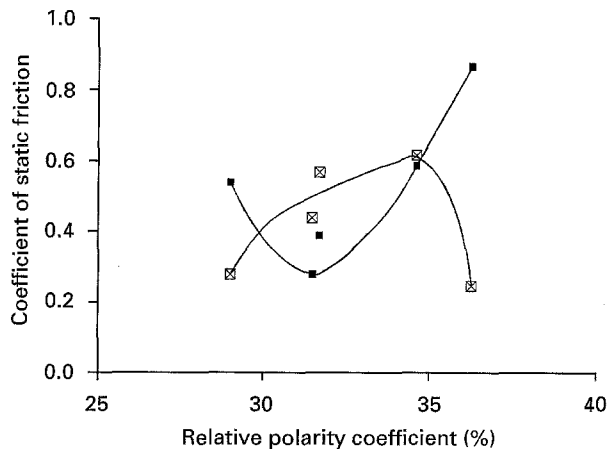


Figure 2 Coefficient of static friction as a function of the relative polarity coefficient, determined on compacted lactose monohydrate (⊠) and salmeterol xinafoate (■) surfaces.

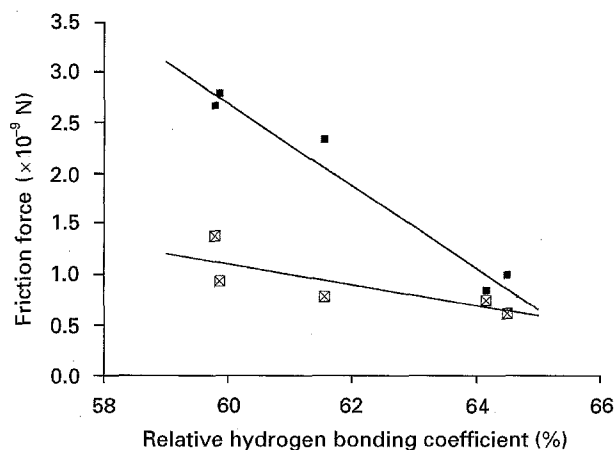
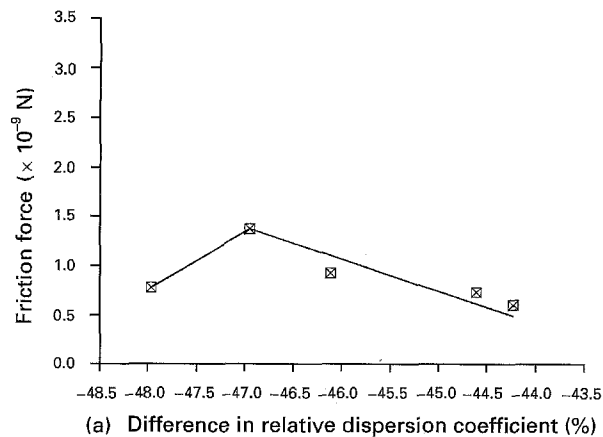


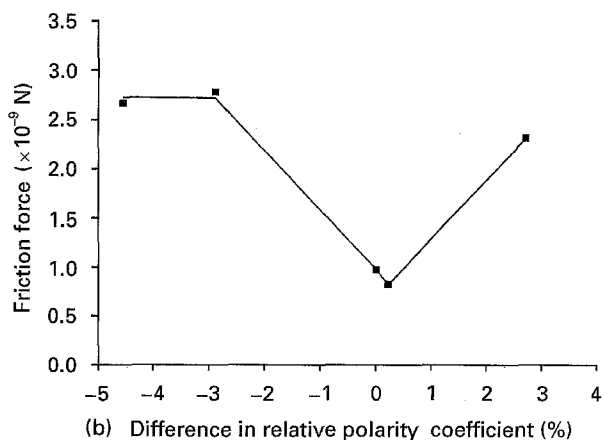
Figure 3 Friction force as a function of the relative hydrogen bonding coefficient, determined on compacted lactose monohydrate (⊠) and salmeterol xinafoate (■) surfaces.

Fig. 3 shows the friction force determined as a function of relative hydrogen bonding coefficient H . There is a clear linear relationship between the friction force and H for salmeterol compounds adhered to compacted lactose monohydrate surfaces. There is also a linear relationship between these particulate materials and compacted salmeterol xinafoate surfaces, but the slope of the latter function is less than obtained on compacted lactose monohydrate surfaces. In both cases, the friction force decreases with increased relative hydrogen bonding coefficient. A larger amount of hydrogen bondings might result in more water being adsorbed on the outside of the particle surfaces. Such water could act as a lubricant between the particles and the surfaces. The compacted salmeterol xinafoate surfaces wet less with water than compacted lactose monohydrate surfaces [16], and therefore the lubricative effect should be less pronounced.

As shown in Fig. 4, there is also a relationship between the friction force obtained on compacted lactose monohydrate surfaces and the difference in the relative dispersion coefficient between the particles and the surface (Fig. 4(a)), and between the friction force obtained on compacted salmeterol xinafoate sur-



(a) Difference in relative dispersion coefficient (%)



(b) Difference in relative polarity coefficient (%)

Figure 4 Friction force as a function of the difference between the relative dispersion coefficient of particles of salmeterol compounds and compacted lactose monohydrate surfaces (a), and between the relative polarity coefficient of particles of salmeterol compounds and compacted salmeterol xinafoate surfaces (b).

faces and the difference between the relative polarity coefficient of the particles and the surface (Fig. 4(b)). This means that for a hydrophilic surface the hydrophobic character of the particulate material adhered dominates the friction process, and vice versa. In both cases an optimum of hydrophilic or hydrophobic character appears to exist. This is very distinctive for the friction of the salmeterol compounds on compacted salmeterol xinafoate surfaces. In fact, friction again appears to be least for like materials in contact (difference between the relative polarity coefficient nearly zero).

Fig. 5 shows that there is an influence of the relative hydrogen bonding coefficient on the shear force between salmeterol particles and a compacted lactose monohydrate surface (Fig. 5(a)), whereas the shear force appears to depend on the relative dispersion coefficient when measured on compacted salmeterol xinafoate surfaces (Fig. 5(b)). In both cases the relationship can be regarded as linear. An increase in relative dispersion coefficient leads to an increase in shear force and presumably to more surface damage during friction on compacted salmeterol xinafoate surfaces. An increase in relative hydrogen bonding coefficient, however, is complemented by a decrease in shear force obtained on compacted lactose monohydrate surfaces, which is in good agreement with the

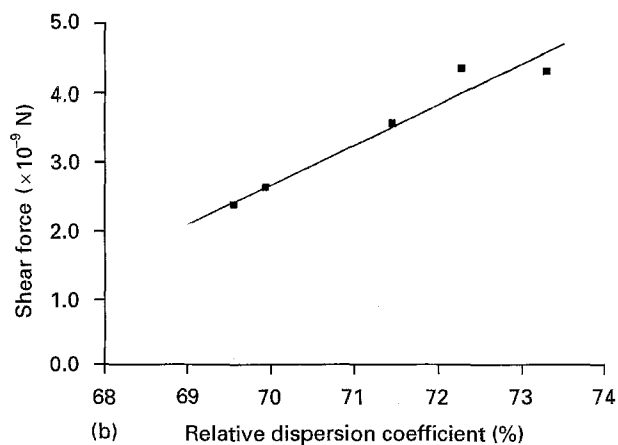
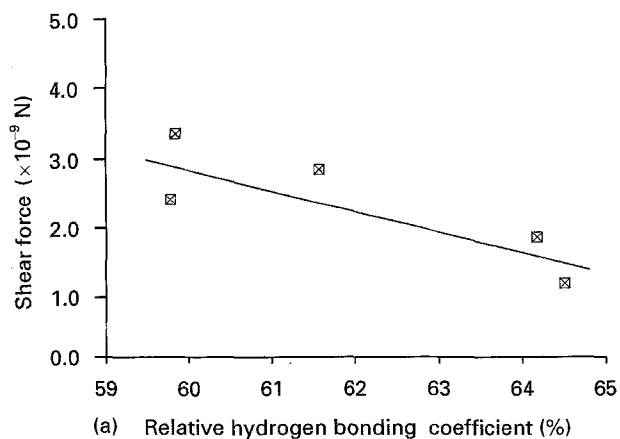


Figure 5 Theoretical shear force as a function of the relative hydrogen bonding coefficient for particles of salmeterol compounds adhered to compacted lactose monohydrate surfaces (a), and of the relative dispersion coefficient of particles of salmeterol compounds adhered to compacted salmeterol xinafoate surfaces (b).

occurrence of stick-slip motion for salmeterol base and sulfate on this surface.

4. Conclusion

The variations in the chemical structure of a series of related compounds could be a key factor to predict adhesion and friction properties on surfaces. However, none of the Hansen-solubility parameters, used in this paper to characterize the chemical structure, can be

regarded as an overall measure of such relationships. Whether or not the hydrophilic or hydrophobic nature of the particles adhered is linked to the friction process depends on the hydrophilic or hydrophobic character of the surface in contact. This implies that there is probably no fixed set of descriptors available, which can always be used to predict or explain a particular friction behaviour. The practical experiment remains therefore the better alternative.

References

1. F. PODCZECK, J. M. NEWTON and M. B. JAMES, *Powder Technol.* **83** (1995) 201.
2. *Idem.*, *J. Mater. Sci.* in press.
3. F. PODCZECK and J. M. NEWTON, *J. Pharm. Sci.* **84** (1995) 1067.
4. I. M. HUTCHINGS, *Powder Technol.* **76** (1993) 3.
5. B. DECELIS, *Wear* **116** (1987) 287.
6. J. A. GREENWOOD and J. B. P. WILLIAMSON, *Proc. Roy. Soc. (London)* **A295** (1966) 300.
7. W. R. CHANG, I. ETSION and D. B. BOGY, *J. Tribology* **110** (1988) 57.
8. F. P. BOWDEN and D. TABOR, "The friction and lubrication of solids", Vol. 2 (Oxford University Press, Oxford, 1964).
9. M. BURDEKIN, N. COWLEY and N. BACK, *J. Mech. Eng.* **20** (1978) 121.
10. K. E. AMIN, *Int. J. Powder Metall.* **23** (1987) 83.
11. G. BÖHME, H. KRUPP, H. RABENHORST and G. SANDSTEDTE, *Trans. Insts. Chem. Engrs* **40** (1962) 252.
12. A. D. ZIMON, "Adhesion of dust and powder", (Consultants Bureau, New York, 1982) pp. 24–30.
13. F. HESLOT, T. BAUMBERGER and B. PERRIN, *Phys. Rev. E* **49** (1994) 4973.
14. H. YOSHIZAWA, Y.-L. CHEN and J. ISRAELACHVILI, *J. Phys. Chem.* **97** (1993) 4128.
15. F. PODCZECK, J. M. NEWTON and M. B. JAMES, *J. Adhesion Sci. Technol.* **8** (1994) 1459.
16. *Idem.*, *ibid.* **9** (1995) 475.
17. F. P. BOWDEN and D. TABOR, "The friction and lubrication of solids", Vol. 1 (Oxford University Press, Oxford, 1950).
18. R. J. ROBERTS and R. C. ROWE, *Int. J. Pharm.* **37** (1987) 15.
19. C. M. HANSEN, *J. Paint Technol.* **39** (505) (1967) 104.
20. C. M. HANSEN and A. BEERBOWER, in "Kirk-Othmer Encyclopedia of Chemical Technology", edited by A. Standen, Suppl.-Vol., (Wiley & Sons, New York, 1971) pp. 889–910.

Received 18 August
and accepted 4 October 1995